


## Article

# Selenium Removal from Aqueous Solution Using a Low-Cost Functional Ceramic Membrane Derived from Waste Cast Iron

Sungmoon Yoon <sup>1,†</sup>, Kang-Hee Cho <sup>2,†</sup>, Minsung Kim <sup>3</sup>, Seong-Jik Park <sup>4</sup> , Chang-Gu Lee <sup>5,\*</sup>  
and Nag-Choul Choi <sup>2,\*</sup>

<sup>1</sup> Green School, Korea University, Seoul 02841, Republic of Korea

<sup>2</sup> Research Institute of Agriculture and Life Science, Seoul National University, Seoul 08826, Republic of Korea

<sup>3</sup> Korea Testing and Research Institute, Ulsan 44412, Republic of Korea

<sup>4</sup> Department of Bioresources and Rural System Engineering, Hankyong National University, Anseong 17579, Republic of Korea

<sup>5</sup> Department of Environmental and Safety Engineering, Ajou University, Suwon 16499, Republic of Korea

\* Correspondence: changgu@ajou.ac.kr (C.-G.L.); nagchoul@snu.ac.kr (N.-C.C.); Tel.: +82-31-219-2405 (C.-G.L.)

† These authors contributed equally to this work.

**Abstract:** The high affinity of iron-based byproducts for anion removal can facilitate wastewater treatment using membranes functionalized with such byproducts. In this study, a low-cost functional ceramic membrane (LFCM) based on waste cast iron (WCI) was fabricated and applied to remove selenium from aqueous solutions. The effect of roasting (1250 °C) on the raw material properties was analyzed by X-ray diffraction and specific surface area measurements. Upon roasting, zero-valent iron (Fe<sup>0</sup>) present in WCI was oxidized to hematite (Fe<sub>2</sub>O<sub>3</sub>), while the specific surface area of WCI increased from 2.040 to 4.303 m<sup>2</sup>/g. Raw WCI exhibited the highest Se(IV) and Se(VI) removal capacity among the prepared materials, and Se(IV) could be removed faster and more efficiently than Se(VI). The selenium removal properties of the synthesized LFCM were similar to those of WCI. This membrane could simultaneously and efficiently remove Se(IV) and turbidity-causing substances through filtration. The results are expected to provide insights into the fabrication of ceramic membranes using industrial byproducts for the removal of ionic contaminants from wastewater.

**Keywords:** ceramic membrane; waste cast iron; selenium removal; adsorption; wastewater



**Citation:** Yoon, S.; Cho, K.-H.; Kim, M.; Park, S.-J.; Lee, C.-G.; Choi, N.-C. Selenium Removal from Aqueous Solution Using a Low-Cost Functional Ceramic Membrane Derived from Waste Cast Iron. *Water* **2023**, *15*, 312. <https://doi.org/10.3390/w15020312>

Academic Editors: Jean-Luc Probst and Alessandro Erto

Received: 30 November 2022

Revised: 25 December 2022

Accepted: 7 January 2023

Published: 11 January 2023



**Copyright:** © 2023 by the authors. Licensee MDPI, Basel, Switzerland. This article is an open access article distributed under the terms and conditions of the Creative Commons Attribution (CC BY) license (<https://creativecommons.org/licenses/by/4.0/>).

## 1. Introduction

Selenium (atomic wt.: 78.96 g/mol) is naturally present in the Earth's crust through weathering, volcanic activities, volatilization of water bodies and plants, and industrial and agricultural activities such as mineral processing, oil refining, fossil fuel use, and pesticide production, which are the dominant sources of anthropogenic pollution [1]. Generally, selenium is an essential micronutrient and good for human health at low concentrations. Because it contributes to reproductive health and thyroid health and helps reduce DNA damage due to its antioxidant properties, the National Institute of Health's Office of Dietary Supplements recommends a daily intake of 55 µg for adults 19 years and above [2,3]. Consumption of more than 400 g of selenium per day, however, might result in undesirable physiological issues such as acute neurotoxicity and chronic endocrine dysfunction [4]. Exposure to excessive selenium may result in gastrointestinal disorders, hair brittleness and discoloration of nails, neurological disorders, and birth deformities [5]. The narrow range (0.8–1.7 mmol/L) between the states of selenium deficiency and selenium toxicity is a subject of concern. Thus, the US Environmental Protection Agency has set a limit of 0.05 mg/L as the maximum selenium contamination level in drinking water [6].

In the environment, selenium can exist in four oxidation states (+VI: selenate, +IV: selenite, 0: elemental selenium, −II: selenide) and several organic forms. Among them, selenite (SeO<sub>3</sub><sup>2−</sup>, Se(IV)) and selenate (SeO<sub>4</sub><sup>2−</sup>, Se(VI)) are the two most common forms of

selenium found in water because the higher valence forms of selenium are more water soluble; additionally, Se(IV) is more toxic than Se(VI) [7]. These two oxyanions are also highly bioavailable and should therefore be removed [8]. There are several methods for removing selenium from water, and these can be categorized into chemical, physical, and biological methods. Interestingly, there is no independent single method ensuring proper treatment; instead, various techniques are combined to achieve the desired water quality at the lowest cost. These technologies include removal techniques such as adsorption, ion exchange, and membrane filtration, as well as conventional techniques such as coprecipitation [9].

Membrane techniques such as nanofiltration and mostly reverse osmosis are effective for removing ionic species like Se(IV) and Se(VI). They rely on hydrostatic pressure-based filtration and separation on micropores with diameters less than 2 nm. The type of membrane used, the type of water to be treated, and the capability of the system to recover play major roles in determining the efficiency of the removal process. The best abatement is achieved using the common cellulose acetate membranes. However, polymeric membranes' poor chemical stability and high propensity for fouling due to their hydrophobic nature can have an impact on both their performance and long-term sustainability [10]. Although reverse osmosis-based techniques are relatively more expensive than nanofiltration, they are much more effective for complete ion removal [9]. The development of novel membranes for selenium removal has remained an interesting research topic. However, the simultaneous achievement of high water permeance and rejection remains a primary challenge with the aforementioned membranes [11].

It is also well known that iron oxides and hydroxides play an essential role in immobilizing selenium in the environment and serve as good adsorbents for the selenium ions in soil and sediments. Due to the strong affinity of iron oxides toward selenium ions, numerous research groups have actively investigated the use of iron-based adsorbents to remove selenium. Considering the advantages of iron, such as low cost and efficient waste material utilization, waste material reuse is increasingly being considered for the preparation of adsorbents [12]. In our previous study, waste cast iron (WCI), a byproduct of the iron casting process in foundries, was used to efficiently extract As(III) and As(V) from aqueous solutions [13]. Thus, WCI is a potential reactive material for treating wastewater. Nonetheless, as far as we know, there is no research on using WCI as a functional material for manufacturing ceramic membranes for water treatment.

Therefore, in this study, a low-cost functional ceramic membrane (LFCM) based on WCI was fabricated and employed for removing selenium from aqueous solutions. The crystal structure changes in the raw materials, including WCI, due to roasting during the ceramic membrane fabrication process were evaluated, and the kinetics of Se(IV) and Se(VI) removal using the prepared samples were compared. The simultaneous removal of Se(IV) and turbidity-causing particles through the LFCM filtration system was also evaluated.

## 2. Materials and Methods

### 2.1. Materials and Chemicals

Alumina powder (AP, AP-400, POS-HIAL, Youngam-gun, Republic of Korea), quartz (K-5, Korsil Co., Asan, Republic of Korea), clay (GF 1250, Duckyu Ceramics Co., Yongin, Republic of Korea), and WCI (Giljin Metals Co., Ltd., Gwangju, Republic of Korea) were used for the fabrication of the LFCM. The stock solution (1000 mg/L), which was prepared using sodium selenate ( $\text{Na}_2\text{SeO}_4$ , 95%, Sigma-Aldrich, Darmstadt, Germany) and sodium selenite ( $\text{Na}_2\text{SeO}_3$ , 99%, Sigma-Aldrich, Darmstadt, Germany), was diluted to appropriate concentrations of Se(IV) and Se(VI). All solutions were prepared and diluted using distilled water (EXL5 U Analysis, Vivagen, Seongnam, Republic of Korea).

### 2.2. Preparation and Characterization of LFCM

The basic composition of the LFCM is given in Table 1. To extrude the alumina-WCI composite support layers for a filtration test, 5 wt.% of methylcellulose ( $[\text{C}_6\text{H}_7\text{O}_2(\text{OH})_x(\text{OCH}_3)_y]_n$ , Sigma-Aldrich, St. Louis, MO, USA) and 13 wt.% of distilled water were added as a binder

and solvent, respectively. A double screw extruder (KTE-50S, Kosentech, Sungnam, Republic of Korea) was used to extrude the mixed slurry after it was aged at room temperature for 48 h. The flat tube-like extruded alumina-WCI composite support layer with 16 interior holes (width: 2 mm; height: 2 mm) was 75 mm wide, 4 mm high, and 62 mm long. After extrusion, the samples were dried at room temperature for 24 h. Then, the dried samples were heat-treated at 400 °C for 1 h and sintered at 1250 °C for 2 h to burn off the binder.

**Table 1.** Composition of the LFCM.

Component	wt. %
Alumina	58
WCI	13
Clay	3
Feldspar	3
Silica	3
Binder	5
Water	13
Glycerin	2
Total	100

Alumina and WCI were also sintered at 1250 °C for 2 h in an electric furnace to confirm the roasting characteristics of the raw materials of the LFCM. X-ray diffraction (XRD, X'pert Pro MRD, Analytical, Almelo, Netherlands) was used to determine the crystallographic properties of the prepared materials, and BET surface area measurement and porosity analysis (ASAP 2010, Micromeritics, Norcross, GA, USA) were performed to determine the specific surface area of the samples. The porosity of the prepared LFCM was measured using a mercury porosity meter (AutoPore IV 9520, Micromeritics, Norcross, GA, USA). The surface morphology of the samples was observed using a scanning electron microscope (SEM, S4800, Hitachi, Tokyo, Japan).

### 2.3. Selenium Removal Experiments

Selenium removal experiments were conducted in batch mode (experiments were conducted in triplicate under ambient conditions). The first set of experiments was conducted to examine the effect of sintering (with or without) on the removal of Se(IV) and Se(VI) using the raw materials (initial selenium concentration = 10 mg/L). The experiments were performed in 50 mL polypropylene conical tubes containing 1.0 g/L of the sample and 30 mL of diluted selenium solution. The tubes were shaken at 30 rpm using a rotary shaker (Daihan Science, Seoul, Republic of Korea). After the desired reaction time (1, 3, and 6 h), the adsorbents were separated from the solution by filtration through a 0.45 µm GFC filter. The residual selenium concentration was measured by atomic absorption spectrophotometry (AAS; Optima-4300, Perkin–Elmer, Waltham, MA, USA).

The removal efficiency of the LFCM was evaluated using synthetic wastewater containing Se and turbidity-causing particles. The Se(IV) concentration in the experiment was 39 µg/L, and 10 g/L of kaolin (size =  $20.20 \pm 38.41$  µm) was used to simulate suspended matter. The experiment was performed by a dead-end membrane filtration method using a flow pump (BT100-2J, Longer, Hebei, China) at a flow rate of 2.76 mL/h. The solution passing through the LFCM was collected every 2 h, and the flow rate, suspended matter, and Se(IV) concentration were measured.

## 3. Results and Discussion

### 3.1. Characterization of Raw Materials

The effect of roasting (1250 °C) on the raw material properties was analyzed by XRD and specific surface area measurement. The XRD patterns of WCI before and after roasting (Figure 1a,b) suggest that zero-valent iron ( $\text{Fe}^0$ ) present in WCI was oxidized to hematite ( $\text{Fe}_2\text{O}_3$ ) upon roasting. Similar oxidation phenomena have been reported in the

literature [14]. Moreover, changes in the crystal structure of iron may also affect selenium removal [12]. In contrast, there was no significant difference in the crystal structure of  $\alpha$ -alumina before and after roasting (Figure 1c,d). After roasting, the specific surface area of WCI increased from 2.040 to 4.303  $\text{m}^2/\text{g}$ , whereas that of  $\alpha$ -alumina decreased from 1.595 to 1.096  $\text{m}^2/\text{g}$  (Table 2). As shown in Figure 2, WCI has an irregular surface morphology, whereas  $\alpha$ -alumina has a relatively smooth surface morphology. In addition, the morphological structure of both surfaces did not change during the roasting (1250  $^{\circ}\text{C}$ ) process.

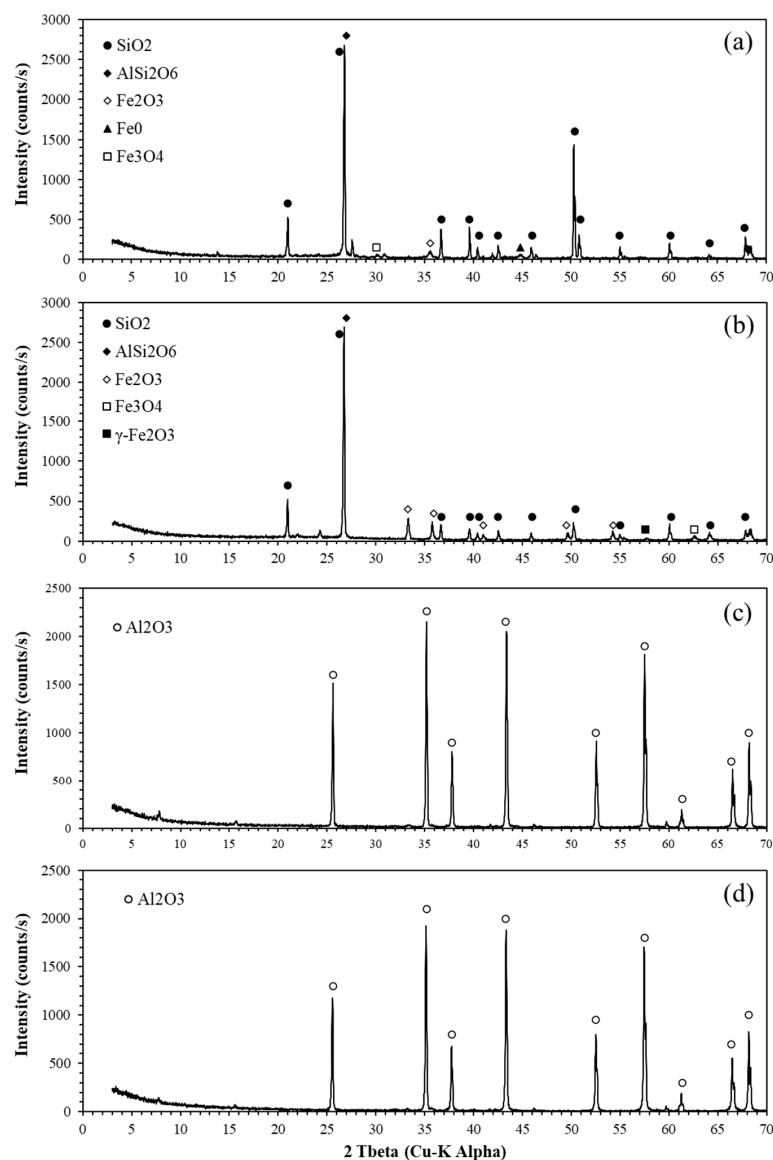


**Figure 1.** XRD patterns of WCI and  $\alpha$ -alumina: (a) raw WCI, (b) WCI after roasting, (c) raw  $\alpha$ -alumina, and (d)  $\alpha$ -alumina after roasting.

**Table 2.** BET surface area of WCI and  $\alpha$ -alumina before and after roasting at 1250  $^{\circ}\text{C}$ .

Sample	Surface Area ( $\text{m}^2/\text{g}$ )
Raw WCI	2.040
WCI after roasting	4.303
Raw $\alpha$ -alumina	1.595
$\alpha$ -alumina after roasting	1.096



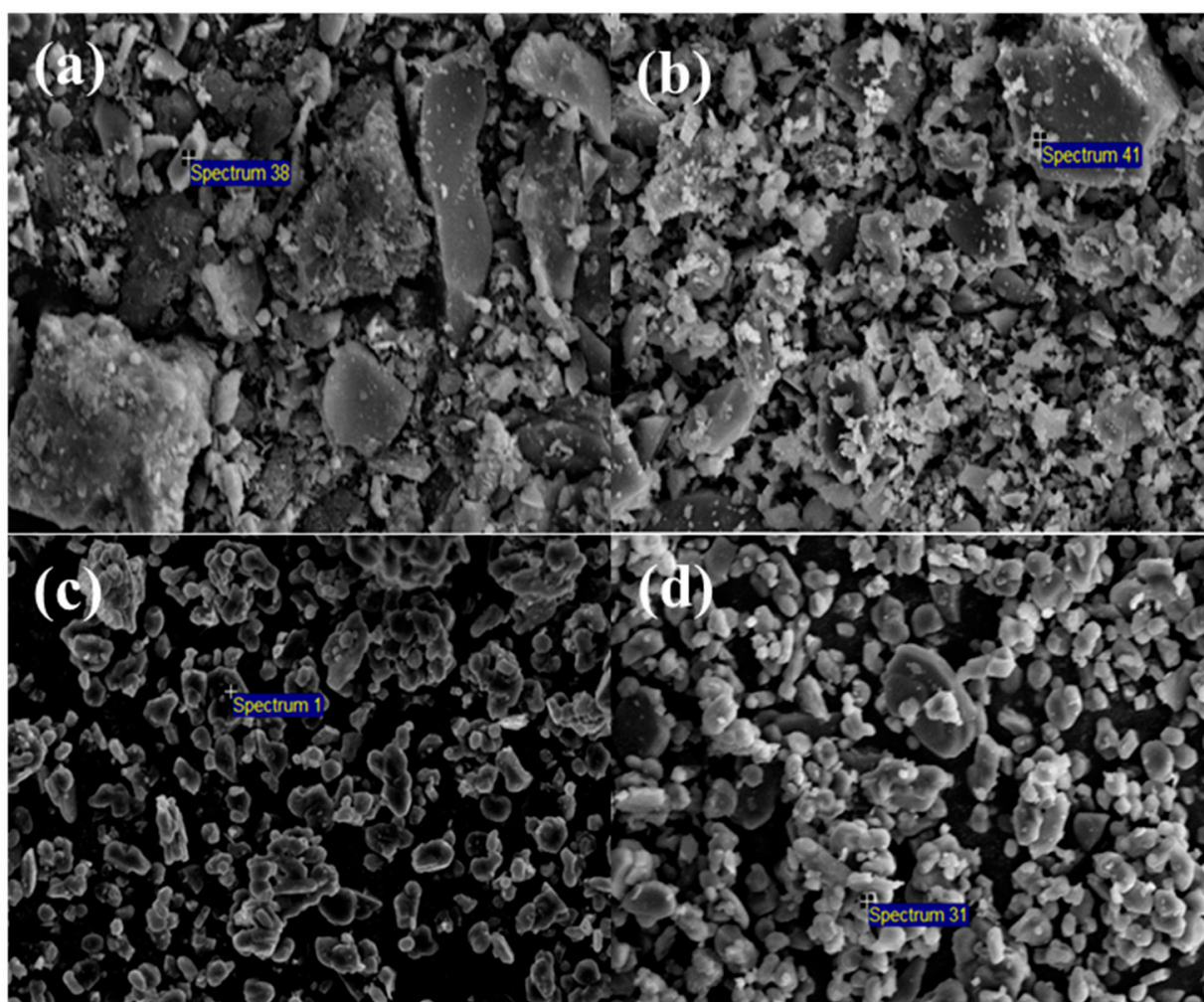


**Figure 2.** SEM images of WCI and  $\alpha$ -alumina: (a) raw WCI, (b) WCI after roasting at 1250 °C, (c) raw  $\alpha$ -alumina, and (d)  $\alpha$ -alumina after roasting at 1250 °C.

### 3.2. Se(IV) and Se(VI) Removal Using Raw Materials

To confirm if the selenium removal performance of the raw materials changed upon roasting during the ceramic membrane fabrication process, selenium removal experiments were performed. As shown in Figure 3, raw WCI had the highest removal capacity among the prepared samples for both Se(IV) and Se(VI). This is because both the magnetite and zero-valent iron ( $\text{Fe}^0$ ) present in raw WCI are effective in removing Se(IV) and Se(VI) [7,12]. As mentioned before, the crystal structure of iron changed upon roasting, thereby leading to a decrease in the selenium removal capacity. This decrease was mainly attributed to the decrease in selenium removal via the reduction mechanism of  $\text{Fe}^0$  present in raw WCI, which was decreased during the roasting process [15]. In contrast, the selenium removal ability of  $\alpha$ -alumina increased for both Se(IV) and Se(VI) after roasting.

Se(IV) and Se(VI) removal reached equilibrium within 1 and 3 h, respectively, after the initiation of the reaction when raw WCI was used (Figure 3). The kinetics of Se(IV) and Se(VI) removal were consistent with a pseudo-first-order kinetic model ( $R^2 > 0.874$ ) [16–19]; the fitted values of the model parameters are listed in Table 3. The faster and better removal of Se(IV) compared to Se(VI) was in good agreement with previously reported results [7,20]. This difference can be attributed to the fact that Se(VI) removal is mainly triggered by inner-sphere complexes, whereas Se(IV) removal is triggered by outer-sphere complexes [21].

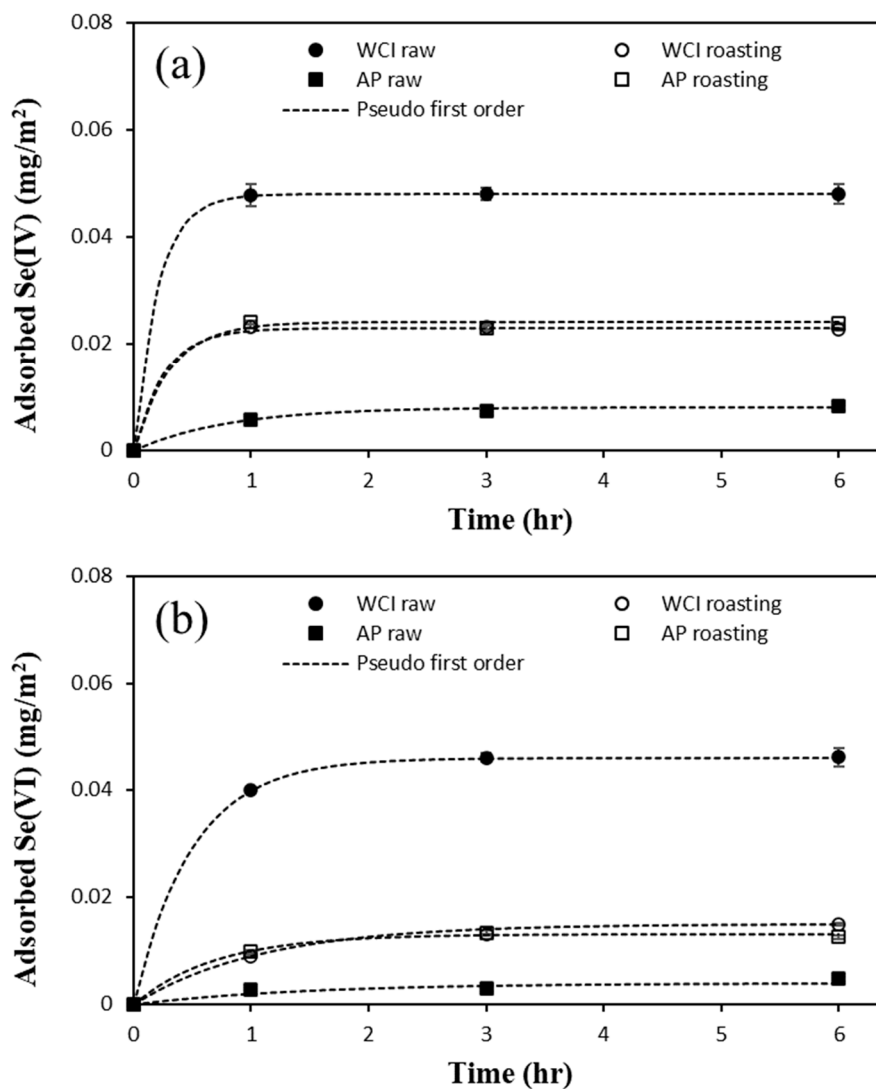


**Figure 3.** Adsorption capacity of (a) Se(IV) and (b) Se(VI) on WCI and  $\alpha$ -Alumina (AP) before and after roasting at 1250 °C.

**Table 3.** Model parameters for the pseudo-first-order kinetic model based on fits to the adsorption kinetic curves.

	Se(IV)			Se(VI)		
	$q_e$ (mg/m <sup>2</sup> )	K (1/h)	R <sup>2</sup>	$q_e$ (mg/m <sup>2</sup> )	K (1/h)	R <sup>2</sup>
WCI raw	0.048	4.875	1.000	0.046	2.016	1.000
WCI roasting	0.023	3.817	1.000	0.015	0.921	0.995
AP raw	0.008	1.251	0.993	0.004	0.688	0.874
AP roasting	0.024	3.234	0.999	0.013	1.439	0.995
LFCM	0.032	3.636	1.000	0.031	0.566	0.926

### 3.3. Characterization of LFCM

The crystallographic structure of the prepared LFCM was analyzed by XRD. Characteristic peaks of quartz (SiO<sub>2</sub>), alumina (Al<sub>2</sub>O<sub>3</sub>), and leucite (AlSi<sub>2</sub>O<sub>6</sub>) could be distinctly observed in the XRD pattern (Figure 4). In addition, peaks corresponding to hematite, magnetite, and maghemite ( $\gamma$ -Fe<sub>2</sub>O<sub>3</sub>), which were originally present in WCI, a raw material for iron, were observed. Because of these iron components, LFCM is expected to be effective in the removal of heavy anionic metals from wastewater, including arsenic and

selenium [7,13,22]. Fe<sup>0</sup>, which was present in WCI, was oxidized during the membrane fabrication process and was considered to be transformed into iron oxide. Pore size distribution analysis of the synthesized LFCM (Figure 5) revealed an average pore size of 0.690 μm and porosity of 44.286%. This corresponds to a value small enough to remove kaolin used to simulate suspended matter.

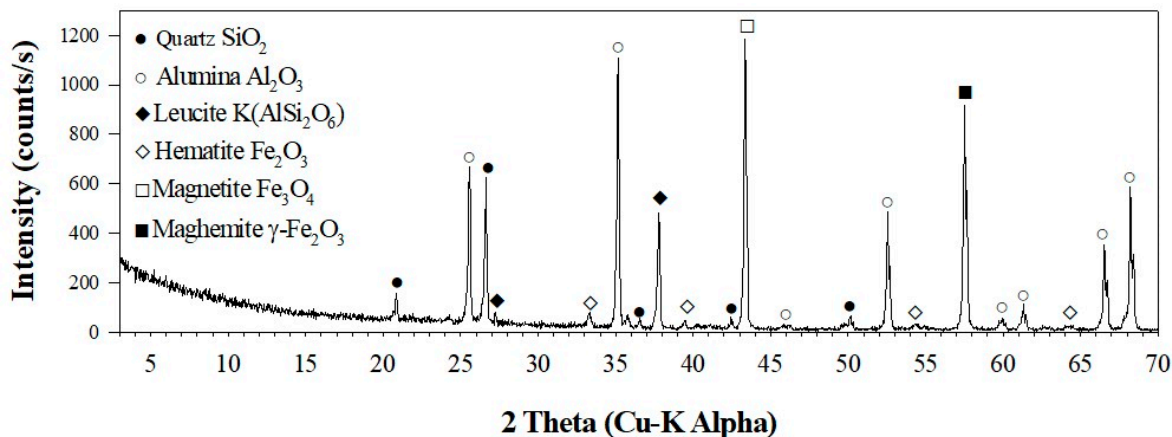


Figure 4. XRD pattern of the LFCM.

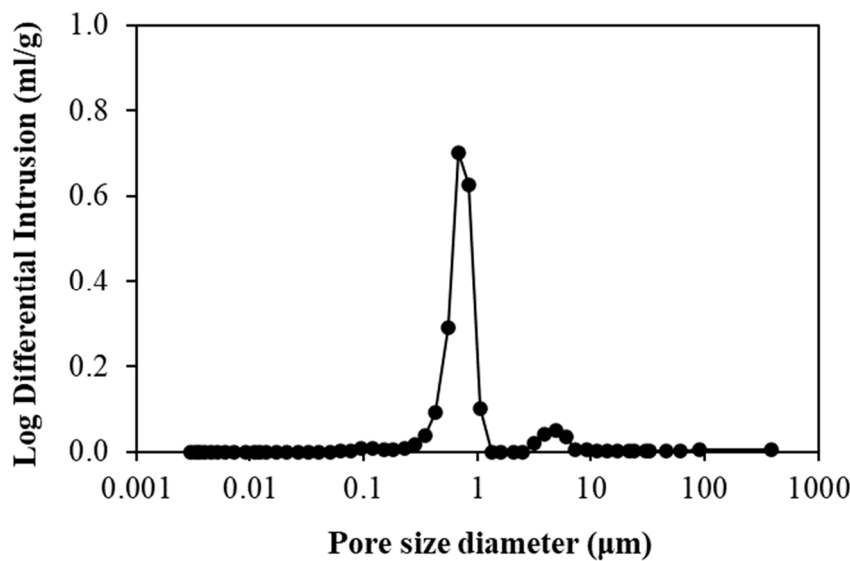


Figure 5. Pore size distribution of the LFCM.

### 3.4. Se(IV) and Se(VI) Removal by LFCM

For comparative evaluation of the performance of the raw material and LFCM, Se(IV) and Se(VI) removal experiments using LFCM were performed under the same conditions. As shown in Figure 6, Se(IV) and Se(VI) removal reached equilibrium within 1 and 3 h, respectively, when LFCM was used. This was the same as the time required to reach equilibrium when the raw materials were used for selenium removal. Thus, the selenium removal capabilities of the raw material and synthesized LFCM were similar but slightly decreased in the synthesized LFCM. Fitting of the kinetic curves to the pseudo-first-order kinetic model ( $R^2 = 0.926$ ) revealed an equilibrium adsorption capacity ( $q_e$ ) and adsorption rate constant ( $K$ ) of 0.032 mg/m<sup>2</sup> and 3.636 /h for Se(IV), respectively, which were higher than those of Se(VI) (Table 3).

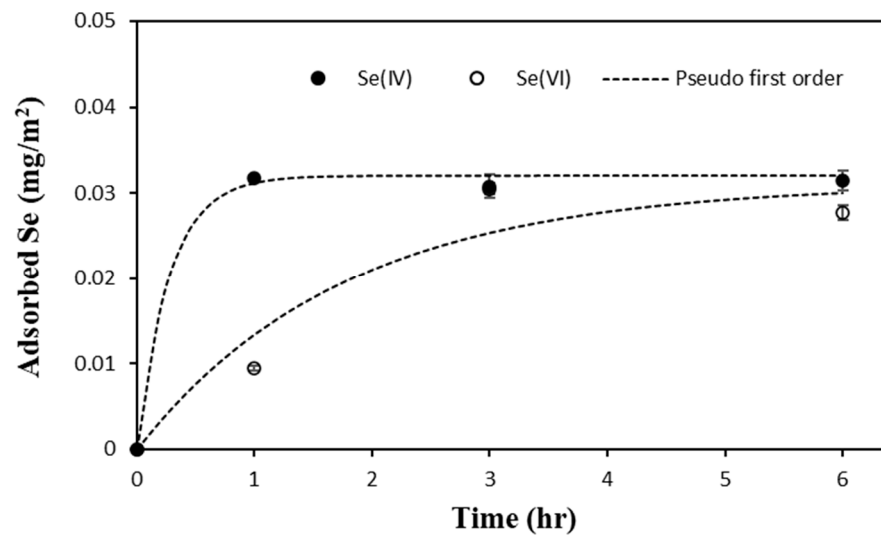


Figure 6. Adsorption capacity of the LFCM for Se(IV) and Se(VI).

### 3.5. Simultaneous Removal of Turbidity-Causing Particles and Se(IV) in the LFCM Filtration System

A filtration experiment was performed using artificial wastewater containing turbidity-causing particles and Se(IV). Kaolin, which was used as a turbidity-causing material, did not leak due to the size exclusion effect of the LFCM filtration system (data not shown). This was consistent with the pore size distribution analysis as well as our previous experimental results [23]. In the case of Se(IV), the breakthrough progressed as the activation sites included in the LFCM were saturated, and the Se(IV) concentration in the effluent was close to the inflow concentration ( $C/C_0 = 0.96$ ) after 38 h of operation (Figure 7). The Se(IV) removal capacity of this filtration system was  $0.027 \text{ mg/m}^2$ , which was lower than the equilibrium adsorption capacity calculated before ( $0.032 \text{ mg/m}^2$ ). However, this indicates that Se(IV) can be effectively removed even while the filtration system is operating. Performance degradation in filtration systems under flow conditions compared to batch systems has also been reported in other studies [24,25].

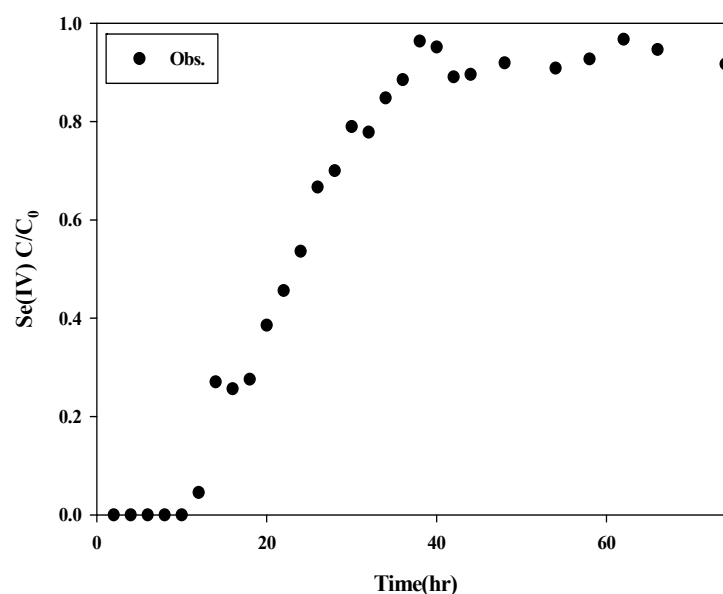


Figure 7. Breakthrough curve of Se(IV) in the LFCM filtration system.



#### 4. Conclusions

In this study, an LFCM derived from WCI was successfully prepared. The iron components present in WCI were oxidized during roasting, which partially lowered the selenium removal capacity. Raw WCI exhibited the highest Se(IV) and Se(VI) removal capacities among the prepared materials, and Se(IV) could be removed faster and more efficiently than Se(VI). The selenium removal properties of the synthesized LFCM were similar to those of WCI, and the former could simultaneously and efficiently remove Se(IV) and turbidity-causing substances through filtration. These results are expected to provide insights into the fabrication of ceramic membranes using industrial byproducts for the removal of ionic contaminants from wastewater.

**Author Contributions:** Conceptualization, N.-C.C.; methodology, S.Y., K.-H.C. and M.K.; validation, S.Y. and K.-H.C.; formal analysis, S.Y. and K.-H.C.; investigation, S.Y. and K.-H.C.; resources, C.-G.L. and N.-C.C.; data curation, C.-G.L. and N.-C.C.; writing—original draft preparation, C.-G.L. and N.-C.C.; writing—review and editing, C.-G.L. and N.-C.C.; visualization, C.-G.L. and N.-C.C.; supervision, S.-J.P.; funding acquisition, C.-G.L. and N.-C.C. All authors have read and agreed to the published version of the manuscript.

**Funding:** This study was supported by a National Research Foundation of Korea (NRF) grant funded by the Korean government (MIST) [grant no. NRF-2021R1F1A1063535].

**Informed Consent Statement:** Not applicable.

**Data Availability Statement:** The data presented in this study are available on request from the corresponding author.

**Conflicts of Interest:** The authors declare no conflict of interest.

#### References

1. Hong, S.H.; Lyonga, F.N.; Kang, J.K.; Seo, E.J.; Lee, C.G.; Jeong, S.; Hong, S.G.; Park, S.J. Synthesis of Fe-impregnated biochar from food waste for Selenium (VI) removal from aqueous solution through adsorption: Process optimization and assessment. *Chemosphere* **2020**, *252*, 126475. [[CrossRef](#)]
2. Burk, R.F. Selenium, an antioxidant nutrient. *Nutr. Clin. Care* **2002**, *5*, 75–79. [[CrossRef](#)]
3. Mojadadi, A.; Au, A.; Salah, W.; Witting, P.; Ahmad, G. Role for Selenium in Metabolic Homeostasis and Human Reproduction. *Nutrients* **2021**, *13*, 3256. [[CrossRef](#)]
4. Lee, N.; Hong, S.H.; Lee, C.G.; Park, S.J.; Lee, J. Conversion of cattle manure into functional material to remove selenate from wastewater. *Chemosphere* **2021**, *278*, 130398. [[CrossRef](#)] [[PubMed](#)]
5. Malhotra, M.; Pal, M.; Pal, P. A response surface optimized nanofiltration-based system for efficient removal of selenium from drinking Water. *J. Water Process. Eng.* **2020**, *33*, 101007. [[CrossRef](#)]
6. Dos Santos, M.; Ramires, P.F.; Gironés, M.C.R.; Rubio Armendáriz, M.d.C.; Montelongo, S.P.; Muccillo-Baisch, A.L.; da Silva Junior, F.M.R. Multiple exposure pathways and health risk assessment of selenium for children in a coal mining area. *Environ. Sci. Pollut. Res.* **2021**, *28*, 13562–13569. [[CrossRef](#)]
7. Lee, C.-G.; Kim, S.-B. Removal of arsenic and selenium from aqueous solutions using magnetic iron oxide nanoparticle/multi-walled carbon nanotube adsorbents. *Desalination Water Treat.* **2016**, *57*, 28323–28339. [[CrossRef](#)]
8. Holmes, A.B.; Gu, F.X. Emerging nanomaterials for the application of selenium removal for wastewater treatment. *Environ. Sci. Nano* **2016**, *3*, 982–996. [[CrossRef](#)]
9. Lichtfouse, E.; Morin-Crini, N.; Bradu, C.; Boussouga, Y.-A.; Aliaskari, M.; Schäfer, A.I.; Das, S.; Wilson, L.D.; Ike, M.; Inoue, D. Technologies to remove selenium from water and wastewater. In *Emerging Contaminants*; Springer: Berlin/Heidelberg, Germany, 2021; Volume 2, pp. 207–304.
10. Asif, M.B.; Zhang, Z. Ceramic membrane technology for water and wastewater treatment: A critical review of performance, full-scale applications, membrane fouling and prospects. *Chem. Eng. J.* **2021**, *418*, 129481. [[CrossRef](#)]
11. He, Y.; Liu, J.; Han, G.; Chung, T.-S. Novel thin-film composite nanofiltration membranes consisting of a zwitterionic co-polymer for selenium and arsenic removal. *J. Membr. Sci.* **2018**, *555*, 299–306. [[CrossRef](#)]
12. Zoroufchi Benis, K.; McPhedran, K.N.; Soltan, J. Selenium removal from water using adsorbents: A critical review. *J. Hazard. Mater.* **2022**, *424*, 127603. [[CrossRef](#)]
13. Choi, N.C.; Kim, S.B.; Kim, S.O.; Lee, J.W.; Park, J.B. Removal of arsenate and arsenite from aqueous solution by waste cast iron. *J. Environ. Sci.* **2012**, *24*, 589–595. [[CrossRef](#)]
14. Monazam, E.R.; Breault, R.W.; Siriwardane, R. Kinetics of Magnetite (Fe<sub>3</sub>O<sub>4</sub>) Oxidation to Hematite (Fe<sub>2</sub>O<sub>3</sub>) in Air for Chemical Looping Combustion. *Ind. Eng. Chem. Res.* **2014**, *53*, 13320–13328. [[CrossRef](#)]

15. Tan, G.; Mao, Y.; Wang, H.; Junaid, M.; Xu, N. Comparison of biochar- and activated carbon-supported zerovalent iron for the removal of Se(IV) and Se(VI): Influence of pH, ionic strength, and natural organic matter. *Environ. Sci. Pollut. Res. Int.* **2019**, *26*, 21609–21618. [[CrossRef](#)]
16. Kang, J.-K.; Park, J.-A.; Kim, J.-H.; Lee, C.-G.; Kim, S.-B. Surface functionalization of mesoporous silica MCM-41 with 3-aminopropyltrimethoxysilane for dye removal: Kinetic, equilibrium, and thermodynamic studies. *Desalination Water Treat.* **2016**, *57*, 7066–7078. [[CrossRef](#)]
17. Meilani, V.; Lee, J.-I.; Kang, J.-K.; Lee, C.-G.; Jeong, S.; Park, S.-J. Application of aluminum-modified food waste biochar as adsorbent of fluoride in aqueous solutions and optimization of production using response surface methodology. *Microporous Mesoporous Mater.* **2021**, *312*, 110764. [[CrossRef](#)]
18. Jang, H.R.; Jeon, H.G.; Moon, D.H. Sorption of Cu, Zn, Pb and Cd from a Contaminated Aqueous Solution Using Starfish (*Asterina pectinifera*) Derived Biochar. *J. Korean Soc. Environ. Eng.* **2021**, *43*, 274–285. [[CrossRef](#)]
19. Kim, J.-H.; Park, J.-A.; Kang, J.-K.; Kim, S.-B.; Lee, C.-G.; Lee, S.-H.; Choi, J.-W. Phosphate sorption to quintinite in aqueous solutions: Kinetic, thermodynamic and equilibrium analyses. *Environ. Eng. Res.* **2015**, *20*, 73–78. [[CrossRef](#)]
20. Okonji, S.O.; Dominic, J.A.; Pernitsky, D.; Achari, G. Removal and recovery of selenium species from wastewater: Adsorption kinetics and co-precipitation mechanisms. *J. Water Process. Eng.* **2020**, *38*, 101666. [[CrossRef](#)]
21. Sun, W.; Pan, W.; Wang, F.; Xu, N. Removal of Se(IV) and Se(VI) by  $MFe_2O_4$  nanoparticles from aqueous solution. *Chem. Eng. J.* **2015**, *273*, 353–362. [[CrossRef](#)]
22. Lyonga, F.N.; Hong, S.-H.; Cho, E.-J.; Kang, J.-K.; Lee, C.-G.; Park, S.-J. As (III) adsorption onto Fe-impregnated food waste biochar: Experimental investigation, modeling, and optimization using response surface methodology. *Environ. Geochem. Health* **2021**, *43*, 3303–3321. [[CrossRef](#)]
23. Choi, N.-C.; Cho, K.-H.; Kim, M.-S.; Park, S.-J.; Lee, C.-G. A Hybrid Ion-Exchange Fabric/Ceramic Membrane System to Remove As(V), Zn(II), and Turbidity from Wastewater. *Appl. Sci.* **2020**, *10*, 2414. [[CrossRef](#)]
24. Chu, J.H.; Kang, J.K.; Park, S.J.; Lee, C.G. Application of the anion-exchange resin as a complementary technique to remove residual cyanide complexes in industrial plating wastewater after conventional treatment. *Environ. Sci. Pollut. Res. Int.* **2020**, *27*, 41688–41701. [[CrossRef](#)]
25. Hong, S.H.; Ndingwan, A.M.; Yoo, S.C.; Lee, C.G.; Park, S.J. Use of calcined sepiolite in removing phosphate from water and returning phosphate to soil as phosphorus fertilizer. *J. Environ. Manag.* **2020**, *270*, 110817. [[CrossRef](#)] [[PubMed](#)]

**Disclaimer/Publisher’s Note:** The statements, opinions and data contained in all publications are solely those of the individual author(s) and contributor(s) and not of MDPI and/or the editor(s). MDPI and/or the editor(s) disclaim responsibility for any injury to people or property resulting from any ideas, methods, instructions or products referred to in the content.